A Geometrical Method for Calculating the Unreachable Workspace of the 3-DOF Gantry-Tau Parallel Manipulator

Ilya Tyapin
The University of Queensland
Brisbane, Australia
Email: ilya@itee.uq.edu.au

Geir Hovland
The University of Agder
Grimstad, Norway
Email: geir.hovland@uia.no

Torgny Brogårdh
ABB Robotics
Västerås, Sweden
Email: torgny.brogardh@se.abb.com

Abstract

One of the main advantages of the Gantry-Tau machine is a large accessible workspace/footprint ratio compared to many other parallel machines. The Gantry-Tau improves this ratio by allowing a change of assembly mode without internal link collisions or collisions between the links and the moving TCP platform. This paper introduces the geometric approach for the unreachable workspace area for the Gantry-Tau. The unreachable area can occur in the middle of the workspace of reconfigurable PKMs with fixed length actuators. It is important to eliminate unreachable areas when designing the Gantry-Tau PKM because they appear in the middle of the workspace which is often the most useful part of the workspace. This approach is significantly faster than analytical workspace calculation methods based on the inverse kinematics. Because of the fast computational speed of the geometric approach, the method is ideal for inclusion in a design optimisation framework. The design presented in this paper achieves a workspace/footprint ratio of more than 2.7 with a zero unreachable workspace. Typical PKMs, for example the Delta robot, has a ratio less than one. In addition, a workspace optimisation method is presented where the parameters are the support frame lengths and the robot's arm lengths.

1 Introduction

A generalised parallel manipulator is a closed-loop kinematic chain mechanism whose end-effector is linked to the base by several independent kinematic chains [Merlet, 2000]. It includes redundant mechanisms with more actuators than the number of controlled degrees of freedom of the end-effector, as well as manipulators working in cooperation. The study of parallel kinematic machines has been an active research field in robotics and mechanical design in recent years. From the first ideas of [Gough, 1957] and [Stewart, 1965], many mechanisms and design methods have been developed. The concept of using the parallel mechanism as a spacial motion mechanism with 6-DOFs was first time presented by [Gough, 1957]. Stewart proposed a 6-DOFs platform targeting its application to a flight simulator. In the late 1980s a new field of applications and research was developed by [Clavel, 1988]. The Delta robot presented by Clavel was a base for a huge range of machines dedicated to high-speed applications but its applications are limited because the degrees of freedom are too small to perform complicated tasks. In contrast, Pierrot proposed a 6-DOF fully-parallel robot HEXA [Pierrot, Uchiyama, Dauchez and Fournier, 1990] and [Uchiyama, Iimura, Pierrot and Dauchez, 1992] which is an extension of the DELTA mechanism. However, the HEXA robot has some disadvantages, including small tilting angle and complexity. Nowadays, industries use parallel mechanisms in wide-ranging applications (drilling, milling, manipulation, packing, assembly processes, motion simulation, pick-and-place, etc.).

The Tau family of parallel kinematic manipulators (PKM) was invented by ABB Robotics, see [1]. The Gantry-Tau was designed to overcome the workspace limitations while retaining many advantages of PKMs such as low moving mass, high stiffness and no link twisting or bending moments. For a given Cartesian position of the robot each arm has two solutions for the inverse kinematics, referred to as the left- and right-handed configurations. While operating the Gantry-Tau in both left- and right-handed configurations, the workspace will be significantly larger in comparison with both a serial Gantry-type robot and other PKMs with the same footprint. The intended application of the robot is for machining operations requiring a workspace equal to or larger than of a typical serial-type robot, but with higher stiffness.

In this paper we consider the triangular-link variant of the 3-degree-of-freedom (DOF) Gantry-Tau structure, which was first presented in [Brogårdh, Hanssen and Hovland, 2005]. Triangular mounted links give several advantages: they enable a reconfiguration of the robot and a larger reach is obtained in the extremes of the workspace. When using parallel links, the orientation of the manipulated platform will be constant, which increases the risk of collisions of the arms with the manipulated platform in the extremes of the workspace area.

In [Johannesson, Berbyuk and Brogårdh, 2004] an optimisation method for the 3-DOF Gantry-Tau with no triangular links was presented. Two geometrical parameters of the machine were optimised to maximise the cross-sectional workspace area. Our paper is an extension of the work in [Johannesson, Berbyuk and Brogårdh, 2004]. The new contributions of this paper are: the optimisation is made for the Gantry-Tau with triangular mounted links, the optimisation is made over the whole workspace volume and not just the cross-sectional workspace area and finally a fully geometric approach to find the unreachable workspace area of the Gantry-Tau is presented and introduced into the design optimisation for the first time.

In order to calculate the workspace one can employ discretisation methods, geometrical methods or analytical methods. For the discretisation method a grid of nodes with position and orientation is defined. Then the kinematics is calculated for each node and it is straightforward to verify whether the kinematics can be solved and to check if joint limits are reached or link interference occurs. The discretisation algorithm is simple to implement but has some serious drawbacks. It is expensive in computation time and results are limited to the nodes of the grid. One example of this approach is [Dashy, Yeoy, Yangz and Chery, 2002].

Analytical workspace area methods which investigate the properties of the kinematic transmission are described in [Angeles, 1985], [Goldenberg, Benhahib and Fenton, 1985]. Most approaches are based on the inverse kinematics because it can typically be solved in closed form and it is easer to distinguish between multiple solutions. Whereas discretisation methods are based on the full inverse kinematics, the analytic approaches usually only require parts of the inverse kinematics. Even so, analytical methods can be expensive in computation time.

Using geometrical methods the workspace can be calculated as an intersection of simple geometrical objects [Merlet, 2000], for example spheres. The midpoints of the spheres are found from the pivot points for example PUS (prismatic joint, universal joint, spherical joint) and UPS (legs form a cylinder and a sphere). Constraints on the joints and on the articulated coordinates can be introduced through further restrictions on the geometrical entities and the intersection of these objects can be done with techniques that are known from computer aided design (CAD). Examples of such constraints are floors, ceilings and prismatic joint locations to avoid collisions with the links.

The works presented in [Chablat and Wenger, 2003], [Liu, Wang and Gao, 2000] and [Tyapin, Hovland and Brogårdh, 2006] are examples of partial geometric approaches to calculate the workspace of a 3-DOF PKM. They are only partial geometric because numeric integration is used to calculate the workspace. However, these authors only considered the reachable and not the unreachable workspace. Design optimisation was attempted by [Chablat and Wenger, 2003], [Liu, Wang and Gao, 2000] and [Tyapin, Hovland and Brogårdh, 2006]. In addition, [Liu, Wang and Gao, 2000] presents the relationships between the workspace and link lengths of all planar 3-DOF parallel manipulator.

Another interesting work is the paper by [Kim, Chung and Youm, 1997]. In that paper a fully geometric approach to calculate the reachable workspace was presented for a 6-DOF Hexapod type PKM. The differences compared to our paper are the use of variable link lengths instead of fixed actuators at the robot base and no design optimisation to reduce the unreachable workspace was attempted in [Kim, Chung and Youm, 1997]. In addition, a fully geometric approach to calculate the reachable workspace area with variable link lengths was presented in [Tyapin, Hovland and Brogårdh, 2007a], but no design optimisation to reduce the unreachable workspace was attempted. In [Tyapin, Hovland and Brogårdh, 2007b] the partial geometric approach to optimise the unreachable workspace of the Gantry-Tau was developed. The differences compared to this paper are the use of a previous kinematic design and integration to calculate the workspace area. The closest work to this paper was presented in [Bonev and Ryu, 2001], but both [Kim, Chung and Youm, 1997] and [Bonev and Ryu, 2001] use an inverse kinematics (rotational matrix) to define a workspace. Most researchers use a basic inverse kinematics (rotational matrix) or Jacobian matrix as a part of a geometric approach to define a workspace.

In our paper the unreachable workspace area is defined as a set of simple geometrical shapes (segments of a circle, triangles, polygons). All calculations are based on cross-points between basic 2D geometrical figures (line, circle, polygon). A geometrical method for the Gantry-Tau that uses parameterisation of the midpoints of the three spheres that intersect at the TCP is used. The geometric approach developed in this paper also handles the fact that the platform orientation is not constant, which is also a difference from most of the existing published work. Section 2 briefly describes the kinematics

and the configuration of the triangular-link version of the Gantry-Tau. The geometric method for the unreachable workspace area is described in Section 3. Finally, the optimisation problem is formulated in Section 4 and results are presented in Section 5.

2 Kinematic Description

In this paper we consider the triangular-link version of the Gantry-Tau structure with fixed arm lengths, which is illustrated in Fig. 1 and Fig. 2.

The 3-DOF Gantry-Tau is a reconfigurable PKM and the architecture consists of a fixed base and a mobile platform connected by three legs. Fig. 1 shows the PKM structure in both the left-handed and right-handed configuration (also called assembly modes). As for the basic Gantry-Tau structure, the position of one end of each of the three parallel arms (fixed lengths L_1, L_2 and L_3) is controlled by a linear actuator with actuation variables q_1, q_2 and q_3. L_i are the arm lengths according to Fig. 1. The actuators are aligned in the direction of the global X coordinate. The arm connected to actuator q_1 consists of one single link. The arm connected to actuator q_2 consists of two parallel links. The arm connected to actuator q_3 consists of three links, where two links are mounted in a triangular configuration. The structure and kinematics of the Gantry-Tau have been presented before, for example in [Brogårdh, Hanssen and Hovland, 2005], [Murray, Hovland and Brogård, 2006], [Williams, Hovland and Brogårdh, 2006]. The actuator track locations are fixed in the Y and Z directions and the locations are denoted T_{1y}, T_{1z}, T_{2y}, T_{2z}, T_{3y} and T_{3z}, respectively. The dimensioning of the PKMs support frame in the case it is symmetric is given by the two variables Q_1 and Q_2 as illustrated in Fig. 1, where Q_1 is the depth and Q_2 is the height. The width of the machine in the X direction is given by the length of the actuators.

Fig. 3 shows the manipulated platform and the fixed kinematic parameters of the moving platform, which are not included in the design optimisation. The points A, B, C, D, E and F are the link connection points. The arm with one single link connects the actuator q_1 with platform point F. The arm with two links connects actuator q_2 with the platform points A and B. The arm with three links connects actuator q_3 with the platform points C, D and E. The triangular pair is connected to points C and E.

Fig. 4 shows the constant platform parameters, where L_p is the platform length, R_p is the platform radius, L_{tool} is the tool length, L_{pin} is the length from the platform circle of radius R_p to the connection point for the universal joints and L_b is the length from the connection point to the center of the joint. A_z and F_y are the Z and Y coordinates in the TCP coordinate frame of two connection pins on the platform. The single link with length L_1 is connected to the pin F via a universal joint pin, while one of the links with length L_2 is connected to the point A. A prototype of the 3-DOF Gantry-Tau with a triangular-mounted link pair built at the University of Agder (Norway) is shown in Fig. 2.

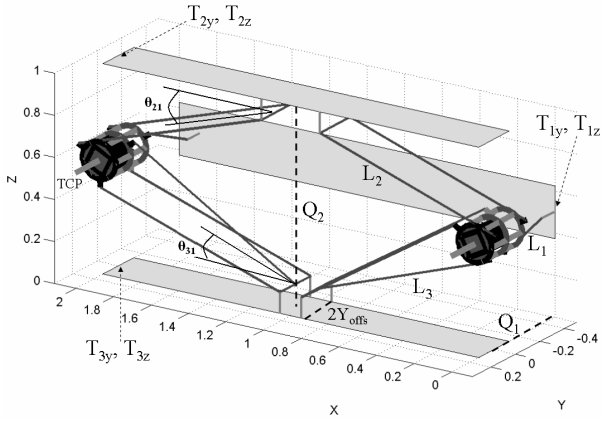

Figure 1: The 3-DOF reconfigurable Gantry-Tau robot.

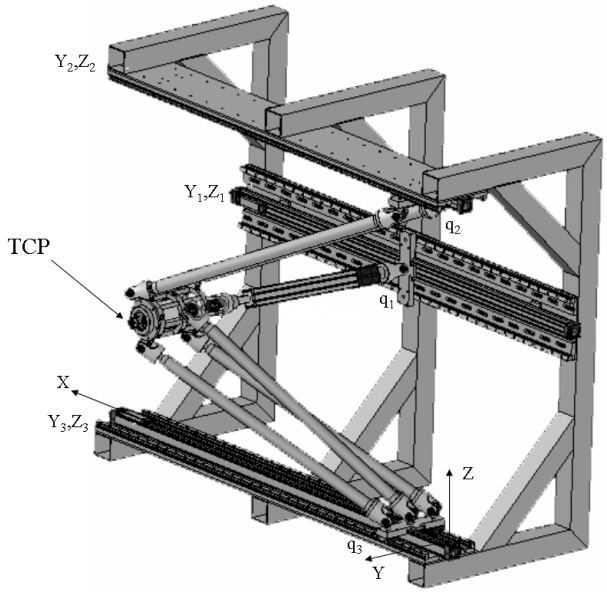

Figure 2: Prototype of a 3-DOF Gantry-Tau with a triangular-mounted link pair.

3 Unreachable Workspace Area and Volume Functions

The cross-sectional workspace of the Gantry-Tau in the YZ-plane is defined from two distinct areas. The first is the maximum boundary of the area which can be reached by the TCP and is denoted as the reachable workspace.

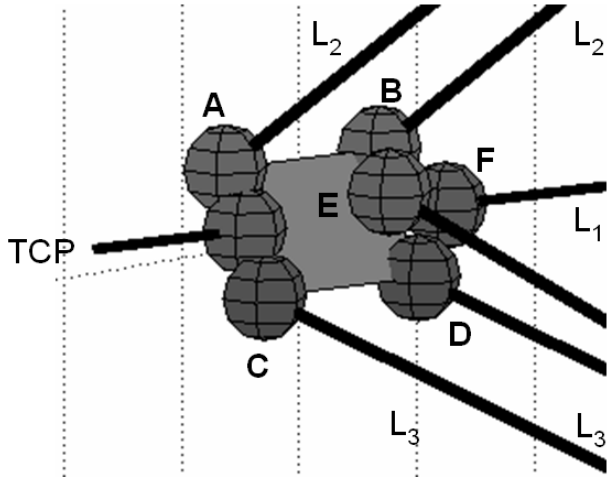

Figure 3: Illustration of platform coordinate points $A - F$.

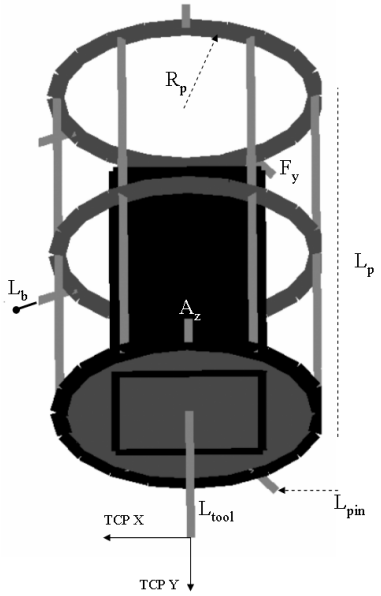

Figure 4: The manipulated platform of the Gantry-Tau robot.

Geometric and partial geometric calculation methods to find this workspace were described in [Tyapin, Hovland and Brogårdh, 2006] and [Tyapin, Hovland and Brogårdh, 2007a]. The reachable workspace in the YZ-plane is illustrated by the shaded region in Fig. 5 and is found from the intersection of three circles with centers at the actuator positions. The numbers 1, 2, 3 in the figure refer to the actuator locations. Actuator 1 has a single link attached, actuator 2 has two links attached and actuator 3 has the remaining three links attached. The three solid lines in the figure illustrate the locations of the support frame which limit the workspace in the positive Z direction and the negative Y direction. The second area is denoted as the unreachable workspace. The unreachable workspace area occurs for PKMs which can change assembly mode and usually occurs in the middle of the workspace. The unreachable workspace area appears when at least one actuator position is at its limit, see Fig. 6. Fig. 6 shows the Gantry-Tau in two different assembly modes and the actuator limits were chosen at $X_L = 0$ and $X_H = 1$. With link lengths larger than $1m$ there is a large unreachable area in the middle of the workspace. The first published work on the unreachable workspace for the Gantry-Tau and a partial geometric approach to minimize the unreachable area was [Tyapin, Hovland and Brogårdh, 2007b].

In Fig. 7, 8 and 9 the unreachable workspace is shown in the YZ-plane in grey color (Fig. 8 and 9). For the figures the actuator limits are $X_L = 0$ and $X_H = 2$ and the link lengths are $1.5m$. The X coordinate of the TCP is $0.7m$ in Fig. 9, $0.6m$ in Fig. 7 and $0.55m$ in Fig. 8.

The geometry of the unreachable workspace is symmetric about the midpoint $x = X_M$ of the linear base actuators. The unreachable area volume is very difficult to be defined as a set of simple geometrical shapes (spheres, cubes, etc.). As a result, the unreachable workspace volume function can be defined as

$$V_U = \sum_{x=X_M}^{x=X_n} 2 \times A_U(x)\delta \tag{1}$$

where δ is the integration step, $A_U(x)$ is the unreachable workspace area for the given X coordinate of the TCP and X_n is the maximum reachable X coordinate of the TCP which has $A_U(x) > 0$. The stages in calculating the unreachable workspace function $A_U(x)$ geometrically are listed below.

Stage 1 : Calculate the intersection points between the circles 1, 2 and 3 as defined in Fig. 5. This stage was described in [Tyapin, Hovland and Brogårdh, 2007a] and is not repeated in this paper. The points are denoted y_{ij}, z_{ij} for the intersection between circle i and j.

Stage 2 : Calculate the radii of the unreachable circles 1, 2 and 3. These circles are defined in Figs. 7 and 8 and are slightly different to the circles in Fig. 5 for the reachable workspace. For circle 1 the center is different because of the platform length, but the radius is the same as in Fig. 5. For circles 2 and 3 the centers are the same as in Fig. 5, but the radii are different because of platform parameters and a dependency on the platform angle α for the circle number 2. The equations for the radii are given in [Tyapin, Hovland and Brogårdh, 2007b].

Stage 3 : Cross-points between three circles will be calculated. The radii of the circles were found in stage 2. The algorithm is the same as used for the reachable workspace in [Tyapin, Hovland and Brogårdh, 2007a].

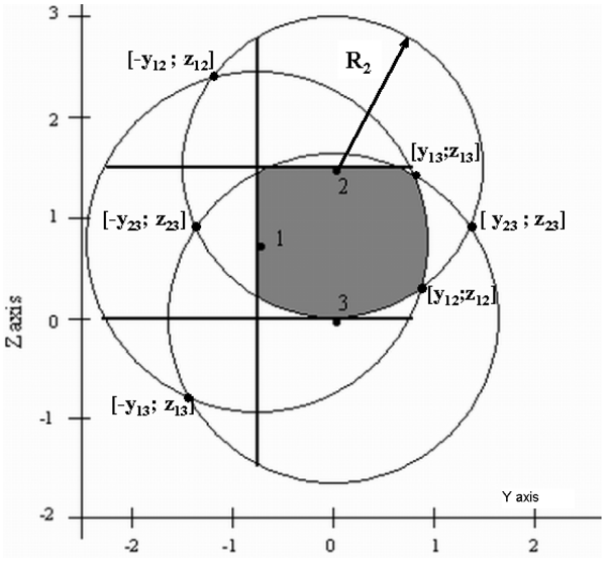

Figure 5: The cross-sectional workspace area of the Gantry-Tau in the YZ-plane.

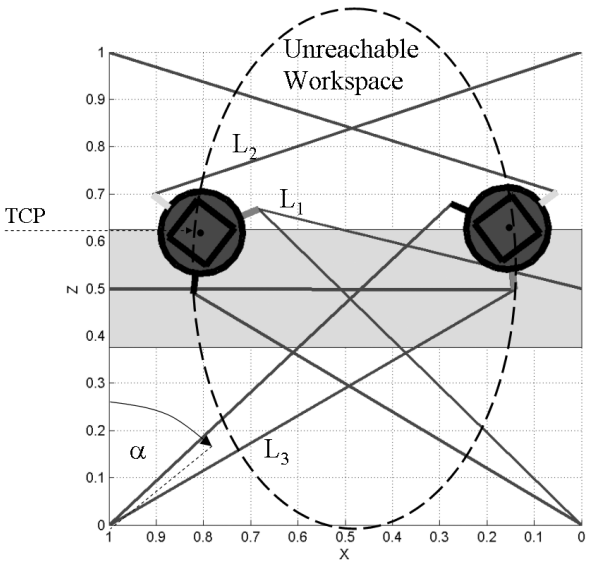

Figure 6: Illustration of unreachable area in the middle of the workspace.

The cross-points for the unreachable workspace are shown in Fig.9, where an index 23 means the cross-point between circle 2 and 3. The subscript $'$ indicates that the point is related to the unreachable workspace. The center of the circle 1 in the YZ-plane is $(T_{1y} + F_y + L_b; T_{1z})$.

In addition, the intersection points between the reachable and unreachable workspace circles will be calculated in this stage, where an index 12 shows the intersection point between the circle 1 from the reachable and the circle 2 from the unreachable workspace. Also, these cross-points have the subscript $''$ before the index and two of them are shown in Fig.9.

Stage 4 : Calculation of the unreachable workspace as a set of simple geometric shapes (segment of circle or polygon). The algorithm consists of two parts: the main solution and one special case if the conditions of the main solution are not satisfied.

The main solution is applicable if circle 1 intersects with the other two circles. Fig. 9 illustrates the unreachable workspace at $x = 0.7$ when arm lengths are $1.5m$, $Q_1 = 0.75m$ and $Q_2 = 1.5m$.

A general test for the main solution with different link lengths and support frame parameters is given below

$$R_2 + R_3 >= Q_2$$

where Q_2 is one of the optimisation parameters and shown in Fig. 1. R_2 and R_3 are radii of the circles 2 and 3 for the given TCP X coordinate. The radii will be defined in stage 2.

In Fig.9 the cross-points $(y'_{12}; z'_{12})$ and $(y'_{13}; z'_{13})$ are outside of the reachable workspace area. The unreachable workspace will be found as a possible reachable

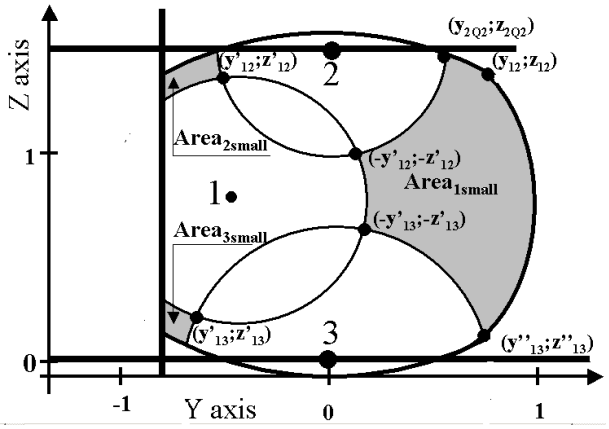

Figure 7: First example of unreachable workspace.

workspace minus the area between points $(y''_{12}; z''_{12})$, $(y''_{13}; z''_{13})$ and $(y'_{23}; z'_{23})$ in Fig.9. The white area between these three points and an area of the $Segment_1$ are the reachable part of the workspace. The unreachable area is shown in grey color in Fig. 9 and given by.

$$A_U = A_{total} - A_{triangle} - A_{segment_1} + ... \quad (2)$$
$$... + A_{segment_2} + A_{segment_3} \quad (3)$$

where A_{total} is the possible reachable workspace area for the given X coordinate and $A_{triangle}$ is the area of a triangle. Three segments of a circle and one triangular area will define the reachable workspace area. All segments can be found from equations presented in [Tyapin, Hovland and Brogårdh, 2007a]. Radii and ends of chords are shown in Fig. 10. However, when the circles will shrink and the circles 2 and 3 will intersect the

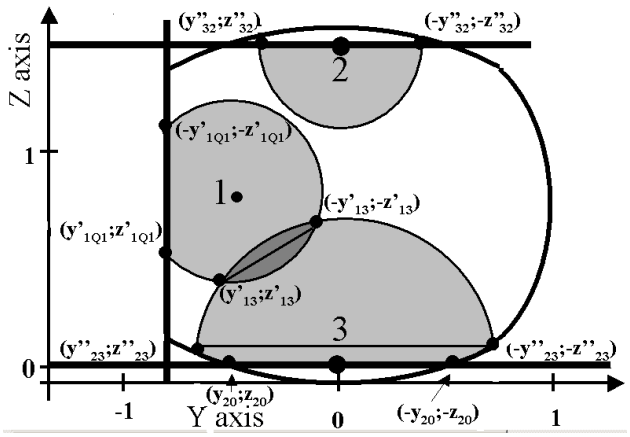

Figure 8: Second example of unreachable workspace.

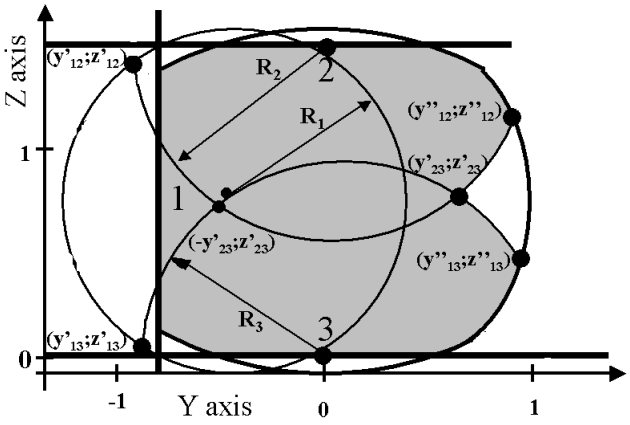

Figure 9: Illustration of unreachable workspace at $x = 0.7$.

circle 1, but not each other, the shape of the reachable workspace will change. A new shape is shown in Fig. 7 and in Fig. 13. Fig. 13 shows 5 segments of a circle and one polygon area. $Segment_1$ has the chord from the cross-point $(y_{12}; z_{12})$ to the cross-point $(y''_{13}; z''_{13})$, the radii equals arm length L_1 and the center is $(T_{1y}; T_{1z})$. $Segment_2$ has the chord from the cross-point $(y''_{13}; z''_{13})$ to the cross-point $(-y'_{13}; -z'_{13})$, the radii equals R_3 and the center is $(T_{3y}; T_{3z})$. $Segment_3$ has the chord from the cross-point $(-y'_{13}; -z'_{13})$ to the cross-point $(-y'_{12}; -z'_{12})$, the radii equals R_1 and the center is the center of the first circle for the unreachable workspace. $Segment_4$ has the chord from the cross-point $(-y'_{12}; -z'_{12})$ to the cross-point $(-y''_{32}; -z''_{32})$, the radii equals R_2 and the center is $(T_{2y}; T_{2z})$. $Segment_5$ has the chord from the cross-point $(-y''_{32}; -z''_{32})$ to the cross-point $(y_{12}; z_{12})$, the radii equals arm length L_3 and the center is $(T_{3y}; T_{3z})$. If the cross-point $(-y''_{32}; -z''_{32})$ is located inside of the circle 1, $Segment_5$ equals 0. The area of the polygon is found from an equation presented in [Tyapin, Hovland and Brogårdh, 2007a]. The unreachable workspace area is given by

$$A_U = A_{total} - A_{polygon} - A_{Segment_1} + A_{Segment_2} + ... \quad (4)$$
$$... + A_{Segments_3} + A_{Segment_4} - A_{Segment_5}$$

All areas are shown in Fig. 13.

In addition, if the circles for the unreachable workspace shrink, cross-points $(y'_{12}; z'_{12})$ and $(y'_{13}; z'_{13})$ (see Fig. 9) will be located inside of the workspace area and two additional reachable areas will be found.

If the cross-point $(y'_{12}; z'_{12})$ is inside of the workspace area, a second part of the reachable workspace area will be defined. The second part is shown in Fig. 7 and Fig. 11. The second part consists of three segments of a circle and one polygon (quadrilateral or triangle).

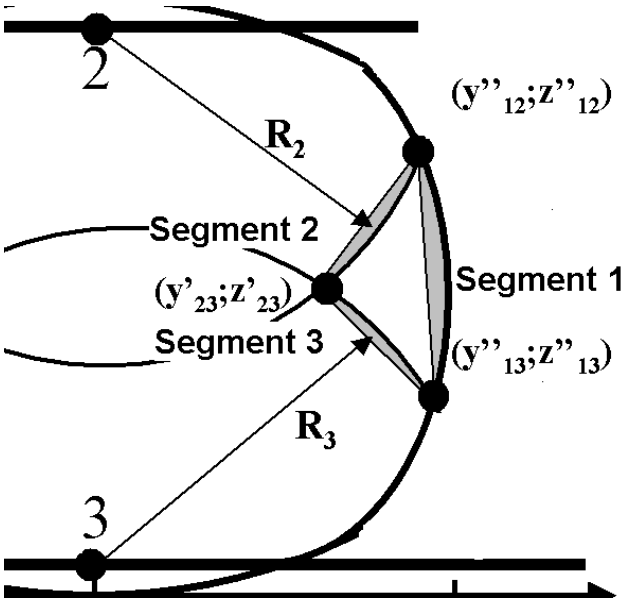

Figure 10: Illustration of a segment of the reachable workspace.

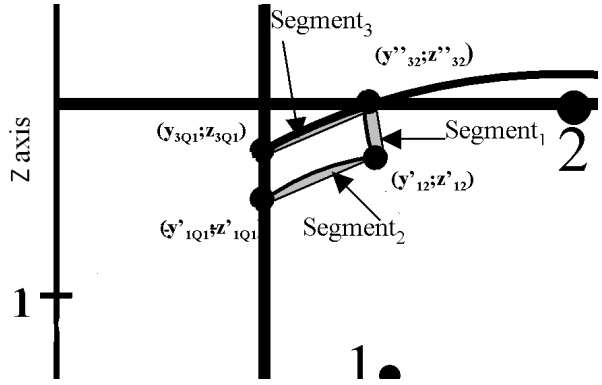

Figure 11: Illustration of a segment of the reachable workspace.

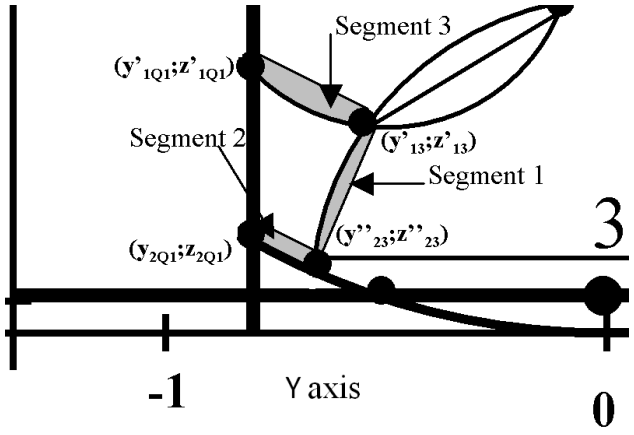

Figure 12: Illustration of a segment of the reachable workspace.

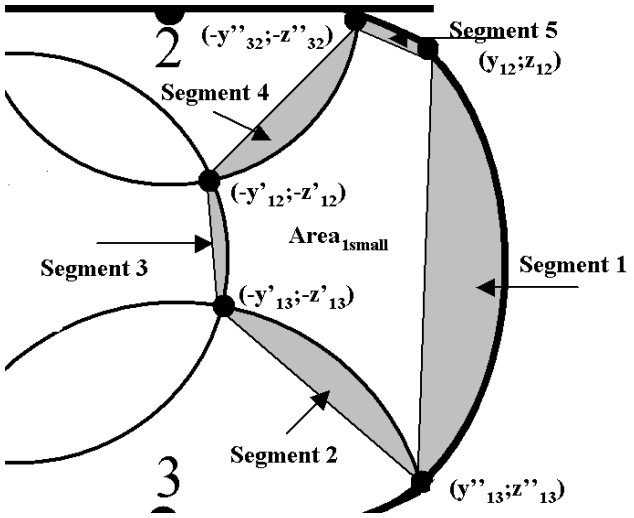

Figure 13: Illustration of a segment of the reachable workspace.

The shape of the polygon depends on the cross-points between the circles and the support frame. If there is no cross-point $(y'_{1Q_1}; z'_{1Q_1})$ or Z-coordinate of this cross-point is greater then Z coordinate of the cross-point between circles 2 of the reachable and 1 of the unreachable workspace, the second part shape will change (three cross-points instead of four). As a result, a polygon will become a triangle $(y''_{31}; z''_{31})(y''_{32}; z''_{32})(y'_{12}; z'_{12})$ and three segments of a circle will be found instead of four.

If the cross-point $(y'_{13}; z'_{13})$ is inside of the workspace area, the third part of the reachable workspace area will be found. The third part is shown in Fig. 7 and Fig. 12. The segment of a circle calculation method was described before in [Tyapin, Hovland and Brogårdh, 2007a]. There are three or four segments of a circle and one polygon (triangle or quadrilateral). Note, that the second and third parts of the reachable workspace will be added in to the unreachable workspace calculation.

In addition to the main solution, there is a special case required for the unreachable workspace calculation if the conditions for the main solution are not met. The special case is applicable if there are no cross-points between unreachable workspace circles or the circle 1 will intersect the circle 2 or 3, but not both of them.

The special case of the unreachable workspace area is shown in Fig. 8 in grey color. There are two segments of a circle between the cross-points $(y'_{13}; z'_{13})$ and $(-y'_{13}; -z'_{13})$. The first segment radii equals R_1, coordinates of a center are $(T_{1y} + F_y + L_b; T_{1z})$, the second segment radii equals R_3 and coordinates of a center are $(T_{3y}; T_{3z})$. If the circles 1 and 2 intersect, but there are no cross-points between the circles 1 and 3, the first and second segments will be found between the circles 1 and 2 in a similar way. $Segment_3$ will be found as a segment of the first circle between points $(y'_{1Q1}; z'_{1Q1})$ and $(-y'_{1Q1}; -z'_{1Q1})$. $Segment_4$ will be found as a segment of circle 2 between points $(y''_{32}; z''_{32})$ and $(-y''_{32}; -z''_{32})$. $Segment_5$ will be defined as a segment of circle 3 with the center in the point $(T_{3y}; T_{3z})$ and the chord $(y''_{23}; z''_{23})$, $(-y''_{23}; -z''_{23})$. If Z coordinates of the chord are greater than the support frame limit, additional segments will be found. In Fig. 8 an extra segment ($Segment_6$) is shown between the chord $(y''_{23}; z''_{23})$, $(-y''_{23}; -z''_{23})$ and the support frame limit $y = T_{3y}$. However, $Segment_6$ consists of two segments: $Segment_{61}$ and $Segment_{62}$, where $Segment_6 = Segment_{61} - Segment_{62}$. $Segment_{61}$ will be found as a segment of the circle 2 between points $(y''_{23}; z''_{23})$, $(-y''_{23}; -z''_{23})$, where the center is $(T_{2y}; T_{2z})$ and radii equals arm length L_2. $Segment_{62}$ will be found as a segment of the circle 2 between points $(y_{20}; z_{20})$, $(-y_{20}; -z_{20})$, where the center is $(T_{2y}; T_{2z})$ and radii equals arm length L_2. The unreachable workspace A_U is finally given by.

$$A_U = Segment_3 + Segment_4 + Segment_5 - ... \quad (5)$$

$$... - Segment_1 - Segment_2 + Segment_6 \quad (6)$$

An extension of the special case is the lack of cross-points between the circles. The unreachable workspace will be found as a set of segments of the circles 1, 2 and 3, where the ends of the chords are the cross-points between the circles and the Gantry-Tau support frame or workspace boundary.

Stage 5: When the total cross-sectional unreachable workspace area in the YZ plane will be calculated as described in Stage 4, the total unreachable volume V_U is calculated numerically by

$$V_U = \sum_{x=X_M}^{x=X_n} 2 \times A_U(x)\delta \quad (7)$$

4 Optimisation Problem

The workspace volume optimisation is based on the least squares nonlinear optimisation function *fmincon* in Matlab. The optimisation problem is expressed as

$$\begin{aligned} &\max V(Q_1, Q_2, L_1, L_2, L_3) \qquad (8)\\ &\text{subject to}\\ &V_U(Q_1, Q_2, L_1, L_2, L_3) = 0\\ &L_1 > 0 \qquad L_2 > 0 \qquad L_3 > 0\\ &Q_1 > 0 \qquad Q_2 > 0 \end{aligned}$$

where V is the normal workspace volume function defined in [Tyapin, Hovland and Brogårdh, 2007a] and V_U is the unreachable volume introduced in this paper and in [Tyapin, Hovland and Brogårdh, 2007b]. The total workspace volume V as a function of the two support frame design parameters Q_1, Q_2 and the individual arm lengths L_1, L_2, L_3 is maximised while keeping the unreachable volume equal to zero. Since the track lengths are fixed and equal to $2.0m$, a unreachable volume will appear if the link lengths become too large. Hence, the unreachable volume is effectively an upper bound on the total achievable workspace when fixed length actuators are used. Without including the unreachable volume in the optimisation problem, it would not be possible to simultaneously optimise both the support frame parameters Q_1, Q_2 and the link lengths L_1, L_2, L_3 as these would all go to infinity.

5 Results

The kinematic parameters of the platform were chosen as follows.

$$\begin{aligned} L_{tool} &= 0.003 \qquad & R_p &= 0.088\\ L_{pin} &= 0.028 \qquad & L_p &= 0.25\\ L_b &= 0.03 \end{aligned}$$

and the support frame parameters were chosen as

$$\begin{aligned} T_{1y} &= -Q_1 \qquad & T_{1z} &= Q_1\\ T_{2y} &= 0 \qquad & T_{2z} &= Q_2\\ T_{3y} &= 0 \qquad & T_{3z} &= 0\\ X_L &= 0 \qquad & X_H &= 2.0\\ Y_{\text{offs}} &= 0.125 \end{aligned}$$

The constrained nonlinear optimisation method in Matlab (*fmincon*) was used and the final optimisation design parameters of the machine were calculated as follows.

$$\begin{aligned} Q_1 &= 0.6426m \qquad & Q_2 &= 0.9947m\\ L_1 &= 0.9987m \qquad & L_2 &= 1.1101m\\ L_3 &= 0.9350m\\ V &= 3.4687m^3 \qquad & V_D &= 0m^3 \end{aligned}$$

These results would have been very difficult to obtain by a manual design, as all the link lengths are different and Q_2 is different from $2Q_1$ which has been a typical manual design choice of the Gantry-Tau in the past, see [Brogårdh, Hanssen and Hovland, 2005] and [Williams, Hovland and Brogårdh, 2006].

The required installation space of the Gantry-Tau equals $(X_H - X_L)Q_1Q_2$ which equals $I = 1.2783m^3$ for the optimised design. Hence, the total workspace to installation space ratio for the optimised design is $\frac{V}{I} = 2.7135$ which is large compared to most other PKMs which typically have a ratio of less than one.

6 Conclusion

In this paper a new geometric approach for describing the cross-sectional unreachable workspace area of the triangular-link version of the Gantry-Tau has been developed. The functional dependency of the cross-sectional workspace area on the robot's x-coordinate is used to calculate the total unreachable workspace volume. In addition to the design parameters, the platform rotation angle α is required to calculate some of the circle radii used in the geometric approach. However, this angle α is not a free variable of the 3-DOF Gantry-Tau and it is easy to calculate, see for example [Williams, Hovland and Brogårdh, 2006].

The geometric approach is typically faster than an approach based on a discretisation of the workspace and using the inverse kinematics to check reachability in each discretised workspace cell. The geometric method returns the exact workspace areas, whereas the accuracy of the discretisation approaches depends on the level of discretisation. If the workspace is discretised more densely to improve accuracy, the computation benefits of the geometric approach increases further. The Table 1 shows the computation requirements for the three different approaches and both the reachable (R.WS) and the unreachable (U.WS) workspace on the triangular version of the 3-DOF Gantry-Tau PKM described in [Brogårdh, Hanssen and Hovland, 2005], [Tyapin, Hovland and Brogårdh, 2006], [Tyapin, Hovland and Brogårdh, 2007b], [Tyapin, Hovland and Brogårdh, 2007a] and [Williams, Hovland and Brogårdh, 2006]. A first approach to calculating the unreachable and the reachable workspace is to use the Jacobian matrix derived from the inverse kinematics and matrix inversion. A second approach was described in [Tyapin, Hovland and Brogårdh, 2007b] and [Tyapin, Hovland and Brogårdh, 2006] and based on a half geometric and numerical method. A third approach was presented in this paper and in [Tyapin, Hovland and Brogårdh, 2007a]. The computing time has been normalised to 1 for the third approach.

Because of the significant computation benefits of the

Method	U.WS, Time	R.WS, Time
Inverse kinematics	34	26
Half numerical	2.4	2.9
Geometric	1	1

(9)

Table 1: Reachable and unreachable workspace volume computation time for three different methods.

geometric approach, this method is far better suited for inclusion in a design optimisation framework compared to discretisation or analytical workspace approaches. The optimised design presented in this paper was obtained in less than an hour on a standard desktop computer using Matlab's Optimisation Toolbox.

The results in this paper show that it is possible to optimise the kinematic design of the Gantry-Tau PKM to achieve zero unreachable workspace while maximising the reachable workspace. The optimised design with no unreachable areas presented in this paper achieves a workspace to footprint ratio of more than 2.7 with fixed length links, which is a very high ratio for a PKM. Typical PKMs, for example the Delta robot, has a ratio less than one.

The main advantage of the developed method is a possibility to change the control cross-points and recalculate the areas using a new data.

Future extensions of the work presented in this paper will introduce performance criteria such as Cartesian stiffness, stiffness rotations and resonance frequencies into the design optimisation.

References

[Gough, 1957] A Platform with Six Degrees of Freedom, Contribution to Discussion to Papers on Research in Automobile Stability and Control and in Tire Perfomance, *Proc. Auto. Div. Institute of Mechanical Engineers*, 1956-1957.

[Stewart, 1965] D. Stewart, A Platform with Six Degrees of Freedom, *Proc. of the 11th World Congress in Mechanism and Machine Science*, 2004.

[Pierrot, Uchiyama, Dauchez and Fournier, 1990] F. Pierrot, M. Uchiyama, P. Dauchez and A. Fournier, A New Design of a 6-DOF Parallel Robot, *Proc. of the 23rd International Sympousium on Industrial Rodots*, pp.771-776, 1990.

[Uchiyama, Iimura, Pierrot and Dauchez, 1992] M. Uchiyama, K. I. Iimura, F. Pierrot, P. Dauchez, K. Unno and O. Toyama, A New Design of a Very Fast 6-DOF Parallel Robot, *Journal of Robotics and Mechatronics*, Vol. 2, No. 4, pp.308-315, 1992.

[Clavel, 1988] R. Clavel, DELTA, a fast robot with parallel geometry, *Proc. of the International Symposium on Industrial Robots*, Lausanne, Switzerland, 26-28 April 1988. pp. 91-100.

[Brogårdh, Hanssen and Hovland, 2005] T. Brogårdh, S. Hanssen and G. Hovland, Application-oriented development of parallel kinematic manipulators with large workspace, *Proc. 2nd International Colloquium of the Collaborative Research Center 562:Robotic Systems for Handling and Assembly*, Braunschweig, Germany, May 2005, pp. 153–170.

[Dashy, Yeoy, Yangz and Chery, 2002] A.K. Dashy, S.H. Yeoy, G. Yangz and I.H. Chery, Workspace analysis and singularity representation of three-legged parallel manipulators *in Proc. of the 7th International Conference in Control, Automation, Robotics And Vision,*, Singapore, 2002, pp. 962-967.

[Brogårdh, 2002] T. Brogårdh, PKM research - important issues, as seen from a product development perspective at ABB Robotics, *Proc. of the Workshop on Fundamental Issues and Future Research Directions for Parallel Mechanisms and Manipulators*, Quebec, Canada, Oct. 2002

[Johannesson, Berbyuk and Brogårdh, 2004] S. Johannesson, V. Berbyuk, and T. Brogårdh, A new three degrees of freedom parallel manipulator, *Proc. 4th Chemnitz Parallel Kinematics Seminar*, Chemnitz, Germany, Apr. 20–21, 2004, pp. 731–734.

[Angeles, 1985] J. Angeles, On the Numerical Solution of the Inverse Kinematics Problem, *Int. J. Robotics Res.*, Vol. 4, no. 2, pp.21-37, 1985.

[Goldenberg, Benhahib and Fenton, 1985] A. A. Goldenberg, B. Benhahib and R. G. Fenton, A Complete Generalized Solution to the Inverse Kinematics of Robots, *Proc. ITEE Journal Robotics Automat*, Vol.RA-1, no. 1, pp.14-20, 1985.

[Hovland, Murray and Brogård, 2006] G. Hovland, M. Murray, and T. Brogårdh, Experimental verification of friction and dynamic models of a parallel kinematic machine, *Proc. of the 2007 IEEE/ASME International Conference on Advanced Intelligent Mechatronics*, Zurich, Switzerland, Sept. 4-7, 2007.

[Murray, Hovland and Brogård, 2006] M. Murray, G. Hovland and T. Brogårdh, Collision-Free Workspace Design of the 5-Axis Gantry-Tau Parallel Kinematic Machine, *Proc. of the 2006 IEEE/RSJ Intl. Conference on Intelligent Robots and Systems,*, Beijing, October 2006.

[Tyapin, Hovland and Brogårdh, 2006] I. Tyapin, G. Hovland and T. Brogårdh, Kinematic Optimisation of the Gantry-Tau Parallel Kinematic Manipulator with

Respect to its Workspace, *Proc. of the Australasian Conference on Robotics and Automation*, Auckland, New Zealand, December, 2006.

[Tyapin, Hovland and Brogårdh, 2007a] I. Tyapin, G. Hovland and T. Brogårdh, A Fully Geometric Approach for the Workspace Area of the Gantry-Tau Parallel Kinematic Manipulator, *Proc. of the 13th IASTED International Conference on Robotics and Applications*, Wurzburg, Germany, August, 29-31, 2007.

[Tyapin, Hovland and Brogårdh, 2007b] I. Tyapin, G. Hovland and T. Brogårdh, Workspace Optimisation of Reconfigurable Parallel Kinematic Manipulator, *Proc. of the IEEE/ASME International Conference on Advanced Intelligent Mechatronics*, Zurich, Switzerland, Sept. 4-7, 2007.

[Merlet, 2000] J.-P. Merlet, *Parallel Robots*, Kluwer Academic Publisher, Solid Mechanics and its Applications, Dordrecht, Boston, Vol. 74, 2000,

[Chablat and Wenger, 2003] D. Chablat and P. Wenger, Architecture Optimisation of a 3-DOF parallel mechanism for machining applications, the Orthoglide, *ITEE Transactions on Robotics and Automation*, Vol. 19, No. 3, pp. 403-410, 2003.

[Williams, Hovland and Brogårdh, 2006] I.Williams, G. Hovland and T. Brogårdh, Kinematic Error Calibration of the Gantry-Tau Parallel Manipulator, *Proc. of the IEEE Intlernational Conference on Robotics and Automation*, Orlando, May 2006.

[Bonev and Ryu, 2001] I. A. Bonev, J. Ryu, A Geometrical Method for Computing the Constant-Orientation Workspace of 6-PRRS Parallel Manipulator, *Mechanism and Machine Theory*, Vol. 36, No. 1, pp. 1, 2001.

[Liu, Wang and Gao, 2000] X.-J. Liu, J.-S. Wang, F. Gao, On the Optimum Design of Planar 3-DOF Parallel Manipulators with Respect to the Workspace, *Proc. of the International Conference on Robotics and Automation*, San Francisco, April, 2000.

[Kim, Chung and Youm, 1997] D.J. Kim, W.K. Chung and Y. Youm, Geometrical Approach for the Workspace of 6-DOF Parallel Manipulators, *Proc. of the IEEE International Conference on Robotics and Automation*, Albuquerque, New Mexico, April, 1997.